Impact of carbonation on chemical and mineralogical properties of stabilized and solidified matrices

Sarra El Bedoui, François Duhaime & Jean-Sébastien Dubé
École de technologie supérieure, Montréal, Québec, Canada
Département de génie de la construction – Laboratoire de géotechnique et de génie géoenvironnemental

ABSTRACT
The purpose of this study is to determine the impact of carbonation, the reaction of atmospheric CO_2 with the cementitious matrix, on the chemical and mineralogical properties of stabilized and solidified (S/S) matrices. The evolution of carbonation with time was followed using thermogravimetric analyses (TGA). X-ray powder diffraction (XRD) allowed the mineral phases of S/S matrices to be identified before and after carbonation. The results showed that carbonation causes the complete and partial transformation of portlandite and C-S-H respectively to calcium carbonate. Geochemical modeling of long-term carbonation of monoliths using PHREEQC showed a decrease in monolith pH, an increase in the calcium, silicon and aluminum concentrations in solution because of the dissolution of the portlandite and the anhydrous tricalcium aluminate and the decalcification of C-S-H. Calcium concentration decreased with acidification of the solution because of precipitation of calcium carbonate. Silicon concentration has been stabilized in acidic medium because of the formation of silica gel by the C-S-H carbonation. The immobilization of lead by carbonation was also shown.

RÉSUMÉ
Le but de cette étude est de déterminer l'impact de la carbonatation, la réaction du CO_2 atmosphérique avec la matrice cimentaire, sur les propriétés chimiques et minéralogiques des matrices stabilisées et solidifiées (S/S). L'évolution de la carbonatation avec le temps a été suivie par des analyses thermogravimétriques (TGA). La diffraction des rayons X (DRX) a permis d'identifier les phases minérales des matrices S/S avant et après carbonatation. Les résultats ont montré que la carbonatation provoque la transformation complète et partielle de la portlandite et du C-S-H respectivement en carbonate de calcium. La modélisation géochimique de la carbonatation à long terme des monolithes en utilisant PHREEQC a montré une diminution du pH monolithique, une augmentation des concentrations en calcium, silicium et aluminium en solution à cause de la dissolution de la portlandite et de l'aluminate tricalcique anhydre et la décalcification des C-S-H. La concentration en calcium diminue avec l'acidification de la solution à cause de la précipitation du carbonate de calcium. La concentration en silicium a été stabilisée à pH faible à cause de la formation de gel de silice par la carbonatation des C-S-H. L'immobilisation du plomb par la carbonatation a également été montrée.

1 INTRODUCTION

Soil contamination has become a major issue that puts human health and wildlife at risk (Chao et al. 2014, Bozkurt et al. 2000).

Currently, there are many remediation methods for contaminated soil that target the extraction or removal of contaminants. On the other hand, the Stabilization/Solidification (S/S) technique, widely applied in the 1970s for the treatment of hazardous waste (Conner 1990), is effective for the immobilization of pollutants, especially inorganic species, and quite economical for use with large volumes of waste (Lange et al. 1996). Based on the use of a hydraulic binder, often Portland cement, S/S physically incorporates contaminants into a hardened mass (solidification) and converts them chemically into less soluble and less mobile forms (stabilization) (Antemir et al. 2010).

However, the long-term performance of the S/S treatment of contaminated soils remains a problem in the remediation of contaminated sites. Indeed, although the short-term effectiveness of this technique has been proven, the long-term durability of monoliths can be affected by alterations, the most significant of which are freeze/thaw, wetting/drying, acid rain and atmospheric carbonation (Antemir et al. 2010; Wang et al. 2016; Song et al. 2006).

The carbonation caused by carbon dioxide present in the air or dissolved in the aqueous phase is considered the most common phenomenon that attacks cementitious materials in the environment and is the subject of this study. It mainly results in the lowering of the pH of the cementitious matrices and the transformation of the principal hydrates of the cement, namely portlandite ($Ca(OH)_2$) and hydrated calcium silicate (C-S-H) into calcium carbonate ($CaCO_3$) (Duprat et al. 2014).

This paper provides a better understanding of the effect of carbonation on chemical composition and on phase changes in S/S monoliths. It also presents the results of the numerical modeling of lead-contaminated monoliths carbonation over the long term using the geochemical simulation code PHREEQC.

2 METHODOLOGY

2.1 Materials

Commercially-available sand (Bomix brand) was used to produce the synthetic S/S monolith. The cement used for the stabilization/solidification treatment of the soil is a GU Portland cement (General Use). Arsenic trioxide (As_2O_3) and lead oxide (PbO) were used to contaminate the S/S

matrices with 31 852 mg/kg of soil and 53 903 mg/kg of soil for As_2O_3 and PbO respectively. Details are given in El Bedoui et al. (2017).

2.2 Preparation of S/S matrices

Two stabilized/solidified matrices each containing an oxide (As_2O_3 or PbO) were produced for this study. They were prepared according to ASTM standard C192-07 (ASTM International 2007). This procedure consists in mixing cement (20%), water (14%), sand (63%) and oxide powders (3%) with a constant Water/Cement ratio (W/C) of 0.7. The mixing proportions for the monoliths contaminated with arsenic and lead are detailed in El Bedoui et al. (2017).

A W/C ratio = 0.7 was used to maximize the capillary porosity (voids between the cement hydrate and anhydrous phases) in order to promote carbonation. The procedure for preparing the two S/S monoliths (the first contaminated with As_2O_3 and the second with PbO) is specified in El Bedoui et al. (2017).

After demolding, the S/S material was cured at high relative humidity for 28 days. Following the cure period, the monoliths were crushed and the particle size of the hydrated material was reduced between 5 and 10 mm. This particle size reduction was done to accelerate carbonation.

2.3 Accelerated carbonation process

In order to produce a carbonated S/S material, the 5-10 mm crushed S/S aggregates were exposed to a CO_2-rich atmosphere. As shown in Fig. 1, the accelerated carbonation consisted in introducing a mixture of air and CO_2 into a series of columns containing the S/S aggregates under constant humidity and temperature.

A CO_2 content of 30 % was retained in this study. In order to study the effect of carbonation as a function of time, 12 carbonation columns were prepared (6 contaminated with arsenic and 6 with lead) with a relative humidity RH = 55 ± 5% (Fig. 1). At predetermined time intervals (0.5, 1, 3, 7, 14 and 28 days), the aggregates samples were removed from two columns (one for As and one for Pb) and stored in air-tight containers for chemical, mineralogical and thermogravimetric analyses.

Non-carbonated samples (put under a nitrogen atmosphere) were necessary to identify the cement hydrates with X-ray diffraction analyses (XRD). They were also used to quantify the initial content of calcium carbonate, the main product of carbonation, and portlandite by thermogravimetric analysis (TGA).

2.4 Thermogravimetric analysis (TGA)

Thermogravimetric analyses were used to determine the portlandite ($Ca(OH)_2$), C-S-H and calcium carbonate ($CaCO_3$) contents in non-carbonated and carbonated matrices (Cazalet, 2012; Scordia, 2008). To perform this test, the aggregates were ground into a fine powder. Before the test, the alumina crucibles were dried and their mass was reset to zero in the thermal analyzer. For each sample, 10 ± 0.1 mg of powder was placed into the crucible, which was installed on its support in the thermobalance. The analysis was conducted under a helium atmosphere.

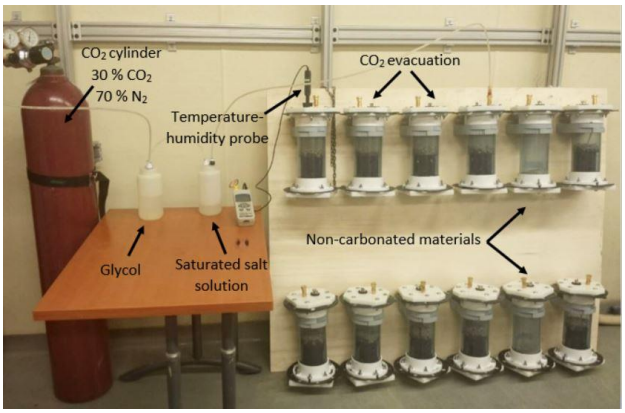

Figure 1. Schematic diagram of the accelerated carbonation device

A linear temperature ramp of 10 °C/min was applied from 29 °C to 1000 °C. During the analysis, the mass loss was recorded as a function of temperature. To ensure the reliability and repeatability of experiments, triplicates were performed on the same ground material. For the material studied in this project, there is no overlap between the loss of water and carbon dioxide (low W/C ratio). As a consequence, a mass spectrometer was not needed to separate these two compounds (Morandeau, 2014).

To better interpret the TGA curves, the raw data was derived and smoothed to obtain the thermogravimetric derived curves (TGD). These curves offer an easier and more accurate reading of the mineral phases degradation temperature ranges as they show sharp peaks which reflect the inflection points of the TGA curves (Thiery, 2006).

In order to quantify the number of moles of portlandite (n_{ch}) and calcium carbonate (n_{cc}) from the TGA results, equations 1 and 2 were used (Morandeau, 2014):

$$n_{ch} = \frac{\%\ H_2O}{M_{H_2O}} \frac{\rho}{100} \quad [1]$$

$$n_{cc} = \frac{\%\ CO_2}{M_{CO_2}} \frac{\rho}{100} \quad [2]$$

% H_2O: Water mass loss associated to CH (determined by the TGA curve)
M_{H_2O}: Molar mass of water
ρ: Density of the monolith
% CO_2: Carbon dioxide mass loss associated with CC
M_{CO_2}: Molar mass of carbon dioxide

2.5 X-ray powder diffraction (XRD)

The qualitative mineralogical analysis of the materials studied was conducted at the Research and Service Unit in Mineral Technology (URSTM) at Université du Québec en Abitibi-Témiscamingue (UQAT). The mineralogy was identified by X-ray diffraction (XRD) using a Bruker AXS D8 advance X-ray diffractometer equipped with a copper anticathode, and scanning over a range of diffraction angle (2θ) from 5° to 70°. Step size for 2θ was set at 0.02 with 4 s counting time per step. DiffracPlus EVA software (v.3.1)

was used to determine mineral phases. The semi-quantification of all minerals was reached with TOPAS software (V4.2) implementing Rietveld refinement. The total accuracy of this quantification method is approximately ±0.5 to 1 wt. % (Bouzahzah et al., 2008).

2.6 Carbonation modeling of monoliths

The purpose of the geochemical modeling is to predict the long-term leaching behavior of contaminants in S/S treated soils as a result of alterations that may attack cementitious matrices, dissolution/precipitation reactions of the various cement phases, and calcium carbonate that is formed over time by carbonation, pH changes, etc (Appelo and Postma, 2005).

The simulation of carbonation of cement hydrates was done using the geochemical code PHREEQC. The default PHREEQC databases are incomplete when describing the chemical reactions of cementitious matrices. This is why the Lawrence Livermore National Laboratory database was used (database llnl supplied with PHREEQC). Additional compounds and mineral phases that characterize the S/S materials and pollutants studied were added using keywords such as SOLUTION_MASTER_SPECIES, SOLUTION_SPECIES and PHASES. The thermodynamic database of Peyronnard (2008) served as a reference to complete the missing information.

An equilibration of the hydrates of the cement with an initial aqueous solution at ambient temperature and pH = 12.49 was made by using the keyword SOLUTION. To simplify the modeling, we put the most important cement hydrates and phases in the model. We introduced portlandite and C-S-H as cement hydrates in the matrix, lead oxide andgypsum and anhydrous tricalcium aluminate to produce ettringite. All these phases were introduced in the form of pure phases (EQUILIBRIUM_PHASES) by indicating their contents and stipulating a saturation index equal to zero in order to impose the thermodynamic equilibrium except for C-S-H. Indeed, since the decalcification of C-S-H is progressive, they were considered as an ideal solid solution (SOLID_SOLUTION) of three C-S-H of different Ca/Si ratio (1.8, 1.1 and 0.8). This gives better results compared to considering the same composition in calcium and silicon for all C-S-H (Stronach and Glasser, 1997). The phases that can precipitate are also introduced into the assembly but with a zero content such as cerussite, hydrocerussite and ettringite. To simulate the progressive diffusion of atmospheric CO_2 in the S/S material in the long term and its reaction with the mineral phases, we used the key words REACTION and INCREMENTAL_REACTION. The gas is then added step by step (step number). This allows us to predict the carbonation of cementitious matrices in the long term.

The geochemical modeling results were compared to the water leaching results of the carbonated samples for 0.5, 1, 3, 7, 14 and 28 days going from the highest pH to the lowest pH. Carbonation for 28 days of S / S materials in the laboratory decreased their pH from 12.24 to 10.7. Since the modeling of carbonation has lowered the pH to 4, which is very difficult to achieve in the field because of the very low CO_2 content in air (0.03-0.06%) (Bertos et al., 2004), it is considered as a long-term simulation.

3 RESULTS AND DISCUSSION

3.1 Thermogravimetric analysis (TGA) results

Thermogravimetric analyses allowed the evolution of carbonation over time to be monitored by quantifying the cement hydrates and calcium carbonate present in the monolith after different contact times.

3.1.1 Arsenic

Pre-carbonation TGA results for the sample contaminated with arsenic are shown in Fig. 2. The TGA and TGD curves correspond respectively to the cumulative mass loss of S/S material phases and the temperature-derivative of this loss. The TGD curve highlights the inflection points that are associated with the decomposition of each mineral phase. The mass loss associated with these inflection points can be used to determine portlandite, C-S-H and calcite contents. For all analyses, the first mass loss occurred between 20 and 400°C. It resulted mainly from the loss of free water and the dehydration of C-S-H and ettringite. The second mass loss was observed between 400°C and 450°C. It was caused by the decomposition of portlandite (CH). The third inflection point occurred between 600 and 700°C. It was the consequence of the decarbonation of the calcium carbonate ($CaCO_3$) produced by carbonation. As shown in Fig. 2, the non-carbonated matrix was rich in cement hydrates (C-S-H, ettrringite and CH). Mass losses of 5%, 1.9% and 1.1% were observed for the dehydration of C-S-H, ettringite and CH respectively. However, the mass loss associated with the decomposition of calcium carbonate was only 0.25%. This small amount of calcite probably comes from the cement or a light carbonation that took place during samples preparation.

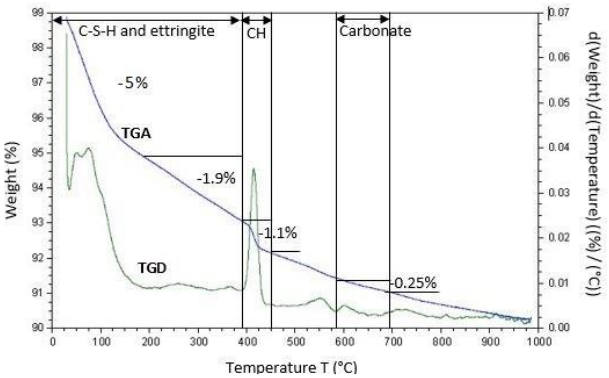

Figure 2. TGA results: Mass loss for the arsenic contaminated matrix before carbonation due to the dehydration of C-S-H, ettringite and CH and the decarbonation of calcite

Figure 3 shows the changes in matrix mineralogy after 0.5, 14 and 28 days of carbonation. Following carbonation, the portlandite peak on the TGD curve became progressively smaller, from 0.0225 %/°C after 0.5 days (Fig. 3a) to 0.005 %/°C after 28 days of carbonation (Fig. 3c). The mass loss for portlandite went from 0.75% (Fig. 3a) to about 0.2% (Fig. 3c) during the 28 days of carbonation. On the other hand, the calcium carbonate TGD peak increased from 0.02 %/°C after 0.5 days of carbonation (Fig. 3a) to 0.095 %/°C (Fig. 3c) after 28 days of carbonation. The mass loss associated with calcium carbonate rose from 1% to 5.3%. As reported previously by Thiery (2006) and Morandeau (2014), this implies that portlandite was the first hydrate to be transformed into calcium carbonate. However, from the 14th day, portlandite depletion was replaced by decalcification of C-S-H to produce calcite. The TGD curve shows the participation of this hydrate to carbonation. Indeed, the TGD peak of C-S-H remained constant (0.035 %/°C) during the first days of carbonation (Fig. 3a), but it then decreased to become 0.025 %/°C on the 14th day (Fig. 3b) and 0.02 %/°C on the 28th day (Fig. 3c).

3.1.2 Lead

The same observations were made for the lead-contaminated matrices. Mass losses of 4.5%, 2%, 1.45% and 0.7% were observed for non-carbonated material for C-S-H, ettringite, CH and calcite respectively (Fig. 4). As with arsenic, carbonation was also supported by the dissolution of C-S-H starting from the 14th day of carbonation, and their transformation into calcite and silica gel when the portlandite content became low which is in agreement with Šavija and Lukovic (2016).

The calculation of portlandite proportions (table 1) indicated that the depletion of this cement hydrate in carbonated S/S matrices was not complete even after decalcification of C-S-H. This is in agreement with Dunster (1989) who showed that, at a relative humidity between 50 and 70%, calcium hydroxide is still present in trace amounts after 80 days of carbonation and the progress of the reaction is sensitive to the particle size. In the long term, the dissolution of C-S-H and $Ca(OH)_2$ is complete: the ultimate degradation state corresponds to a mineral assemblage of calcium carbonate and silica gel (Groves et al., 1990).

Table 1. Amounts of portlandite (CH) and calcium carbonate (CC)

	Amounts of material (mol/L)	
	Arsenic	Lead
n_{CH} NC	1.08	1.48
n_{CH} C	0.19	0.3
n_{CC} NC	0.1	0.29
n_{CC} C	2.14	2.3

Figure 5 shows the evolution of the mineral phase proportions during the 28 days of carbonation. Portlandite (CH) dissolved rapidly during the first 3 days of carbonation, then more slowly. Through 28 days, the portlandite content decreased from 1.08 to 0.19 mol/L for arsenic (nCH-As) and from 1.48 to 0.3 mol/L for lead (nCH-Pb). This hydrate was transformed into calcium carbonate (CC). The amount of CC increased over time from 0.1 to 2.14 mol/L for arsenic and from 0.29 to 2.3 mol/L for lead (Table 1 and Fig. 5). The amount of CC first increased rapidly and then more slowly, thus mirroring the trend for CH.

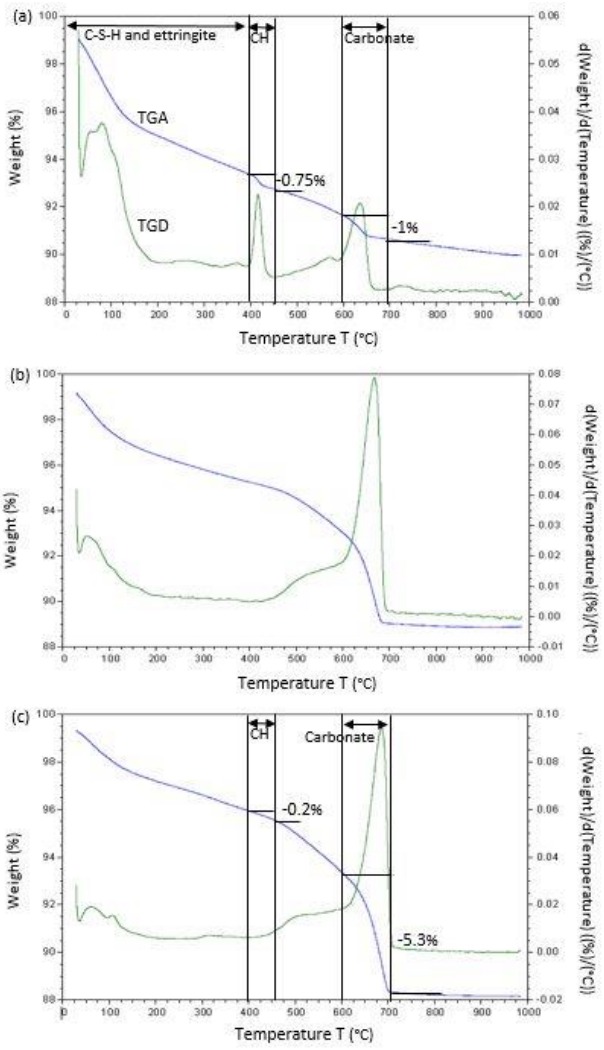

Figure 3. TGA results: Mass loss for the arsenic contaminated matrix due to the dehydration of C-S-H, ettringite and CH and decarbonation of calcite: after (a) 0.5 days, (b) 14 days, (c) 28 days of carbonation

Decalcification of C-S-H began after the 7th day (Fig. 5). The quantity of C-S-H decreased from 4.9 to about 2.6 mol/L for both As and Pb matrices. The onset of C-S-H decalcification is not associated with a break in the trend for calcite content.

TGA results for As and Pb contamination are noticeably similar (Fig. 5). The main difference concerns the carbonates formed in arsenic (nCC-As) and lead (nCC-Pb) matrices. This difference is most likely due to the production of lead carbonate in addition to calcium carbonate in Pb matrices.

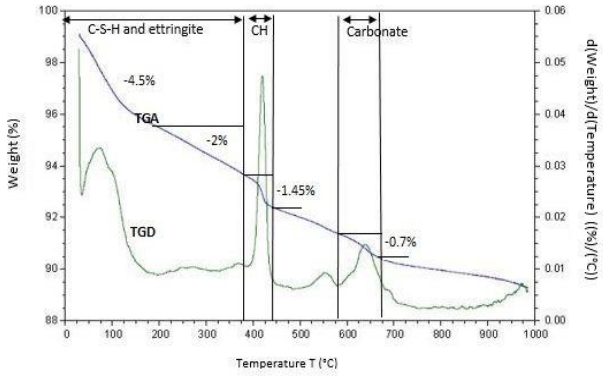

Figure 4. TGA results: Mass loss for the lead contaminated matrix before carbonation due to the dehydration of C-S-H, ettringite and CH and the decarbonation of calcite.

Table 1 shows the amounts of portlandite (CH) and calcium carbonate (CC) calculated from the results of the TGA and equations proposed by Morandeau (2014) for non-carbonated (NC) and carbonated (C) arsenic and lead contaminated matrices. As indicated in this table, NC matrices were rich in portlandite (CH) and low in calcium carbonate (CC) contrary to carbonated monoliths. The amount of the CC formed after carbonation (n_{CC} C) was about 2 mol/L for both arsenic and lead contaminated matrices. Portlandite content (n_{CH} NC) crystallized during the hydration of cement, was about 1 mol/L. As discussed previously, this hydrate was almost completely transformed into calcium carbonate and the production of this mineral was supported by decalcification of C-S-H. Consequently, the difference in amount (about 1 mol/L) was most likely due to the dissolution of the C-S-H.

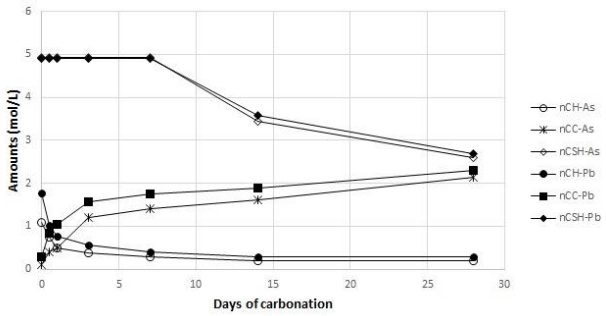

Figure 5. Changes in proportions of CH, C-S-H and CC during the 28 days of carbonation

3.2 Identification of mineral phases by X-ray powder diffraction (XRD)

Even if its results are essentially qualitative, XRD can help to identify and quantify the mineral phases of cementitious materials contaminated with arsenic and lead before and after carbonation. In this case, XRD was used to compare the main phases for non-carbonated and carbonated samples (28 days). Diffractograms for both lead and arsenic contaminated materials are shown in Figs. 6-9.

All diffractograms showed the dominance of quartz, plagioclase (labradorite) and K-feldspar (orthoclase) (Figs. 6-9). These mineral phases are associated with the monoliths' sand component. Some of the minor phases (actinolite, phlogopite and ilmenite) observed on the diffractograms are also associated with sand. All these sand phases displayed similar proportions in both the non-carbonated and carbonated samples, implying that they were not involved in the process of carbonation.

The XRD results clearly showed the main phase change resulting from carbonation: the dissolution of portlandite and precipitation of calcite. Non-carbonated monoliths contaminated with lead (Fig. 6) or arsenic (Fig. 8) were rich in calcium hydroxide (portlandite, CH) with 10.61% and 6.90% respectively and poor in calcite with 4.47% and 3.53% respectively. However, CH was absent in the carbonated materials and the calcite content increased for both lead (Fig. 7) and arsenic (Fig. 9) with 22.93% and 17.58% respectively. This demonstrates the complete transformation of portlandite to calcite during carbonation due to the reaction of cement hydrates, water and CO_2. The presence of calcium carbonate in the non-carbonated matrices can probably be explained by a limited carbonation of portlandite, which took place during sample storage and preparation due to CO_2 in atmosphere. These results are in agreement with previous XRD results on carbonated and non-carbonated cementitious materials (Chen et al., 2009; Antemir et al., 2010; Gunning et al., 2010) and with the TGA results presented in section 3.4.

Small proportions of ettringite were identified by XRD observations after 28 days of carbonation (Figs. 7 and 9). Ettringite was probably formed as a secondary phase after cement hydration. Arsenic and lead compounds were not detected, probably because they did not have sufficient time to develop crystalline structures.

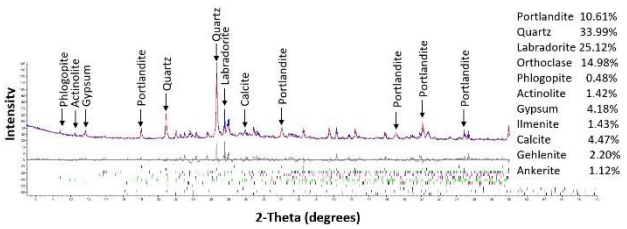

Figure 6. Diffractogram of non-carbonated cement matrix contaminated with lead

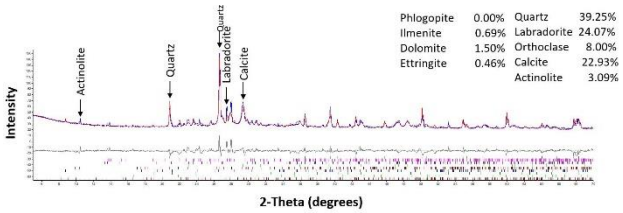

Figure 7. Diffractogram of carbonated cement matrix contaminated with lead

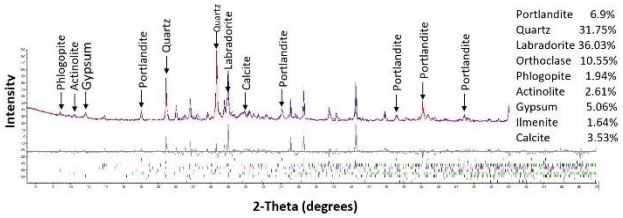

Figure 8. Diffractogram of non-carbonated cement matrix contaminated with arsenic

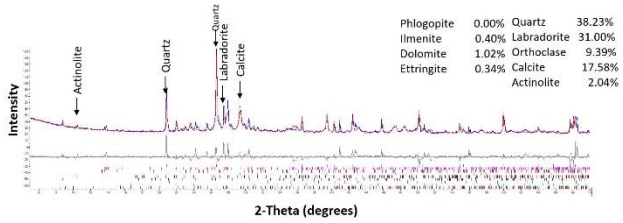

Figure 9. Diffractogram of carbonated cement matrix contaminated with arsenic

3.3 Geochemical modeling of carbonation by PHREEQC

Figures 10 to 15 present some results from the PHREEQC modeling of the carbonation (30% CO_2) of S/S contaminated lead monolith. Validation of the model was done by comparing simulated (full-line) and experimental water leaching results of samples carbonated for 0.5, 1, 3, 7, 14 and 28 days going from the highest pH to the lowest pH (scatter plot). In general, there is an agreement between the two. Figure 10 shows the decrease in pH from 12.46 (initial pH of lead contaminated monolith after S/S treatment) to around 5 as a result of carbonation. However, experimental results of laboratory carbonation for 28 days decreased the pH from 12.46 to 10.7. This acidification of the interstitial solution leads to the dissolution of the hydrates of the cement, the formation of calcium carbonate and the leaching of some elements.

Figure 11 shows the calcium content as a function of pH during carbonation. It shows an increase of calcium in solution with the decrease in pH (between pH = 11.6 and 10.8) because of the dissolution of the portlandite which is the first hydrate to dissolve. As proven previously by TGA results, carbonation is also causes a decalcification of C-S-H thus participating in the release of calcium ions. Then, the calcium content decreases due to its precipitation in the form of calcium carbonate until pH = 6.2 and increases again because of the dissolution of this mineral.

Figure 12 presents the modeling of the impact of carbonation on long-term leaching of lead as a function of pH. The results of water leaching (scatter plot) and nitric acid leaching presented in El Bedoui et al. (2017) showed that carbonation favored the immobilization of lead. Simulation of the solubility of this contaminant has also confirmed the positive effect of carbonation on the behavior of this contaminant. As shown in this figure, lead concentration in the solution greatly decreased with the decrease in pH. The immobilization of lead by carbonation is especially remarkable between pH 6 and 8. This is due to the precipitation of this pollutant in the form of lead carbonate (cerussite: $PbCO_3$). The increase in the concentration of this pollutant from pH = 6 is caused by the dissolution of this mineral.

Figure 13 shows the simulation of aluminum content as a function of pH during carbonation. It is clear that the concentration of this element increases over time with the acidification of the cementitious matrix. This is the consequence of the dissolution of the anhydrous tricalcium aluminate which is one of the initial phases of the cement (introduced as initial pure phase in PHREEQC). Then, its concentration stabilizes from pH 6 because of the precipitation of this compound in the form of ettringite following the hydration of the aluminate by the water released by the phenomenon of carbonation.

The solubility of silicon as a function of the pH during carbonation is shown in Figure 14. The concentration of this compound increases with the decrease of the basicity of the cementitious matrix. This is due to the dissolution of C-S-H to form calcium carbonate following the diffusion of CO_2 in the cement matrix (El Bedoui et al., 2017). The carbonation of C-S-H also leads to the formation of silica gel (Bonen and Sarkar, 1995) leading to a constant concentration of silicon in solution in acidic medium (formation of a plateau from pH 9.5).

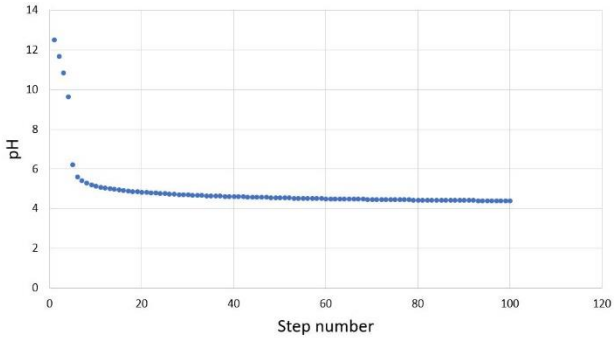

Figure 10. Simulation of the pH decrease following carbonation

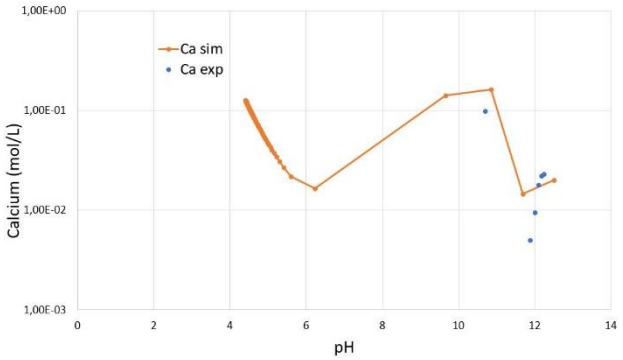

Figure 11. Simulation of the solubility of calcium following carbonation

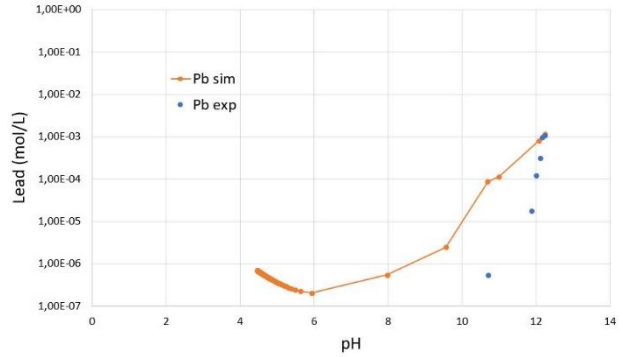

Figure 12. Simulation of the solubility of lead following carbonation

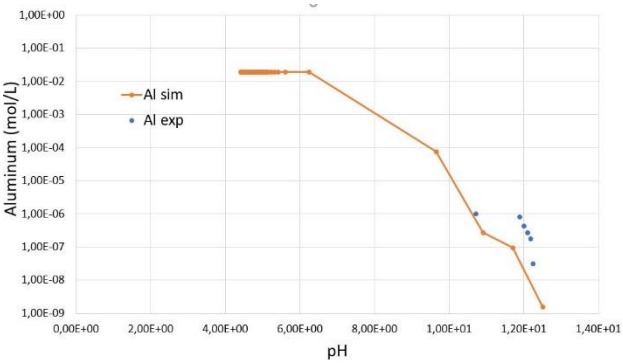

Figure 13. Simulation of the solubility of aluminum following carbonation

We also simulated the dissolution/precipitation of C-S-H following carbonation (Figure 15). A positive saturation index (SI) indicates a precipitation reaction whereas a negative index indicates a dissolution reaction. As can be seen in this figure, the IS of C-S-H 1,8 (calcium rich) is -100 at basic initial pH. This means that this cement hydrate has undergone a strong dissolution. Then, the reaction rate decreases (IS zero between pH 8 and 12) and increases again at pH <8 but in a moderate way. C-S-H 1,1 (moderately rich in calcium) were also dissolved, but to a lesser extent and only from pH <8 (IS between -10 and -12). The dissolution of these two types of Ca/Si hydrates results in the precipitation of C-S-H 0,8 (calcium-depleted), the content of which was initially set to zero in the PHREEQC script. This phase also undergoes dissolution at acidic pH (IS between -8 and -10).

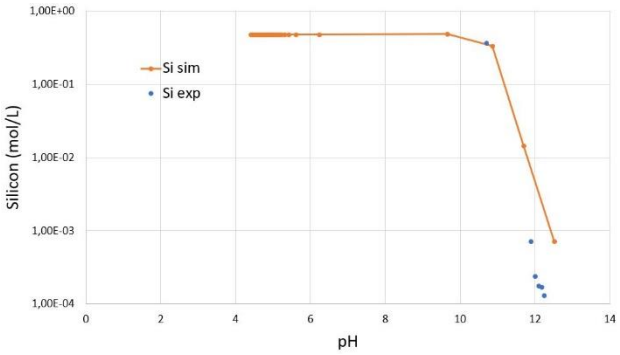

Figure 14. Simulation of the solubility of silicon following carbonation

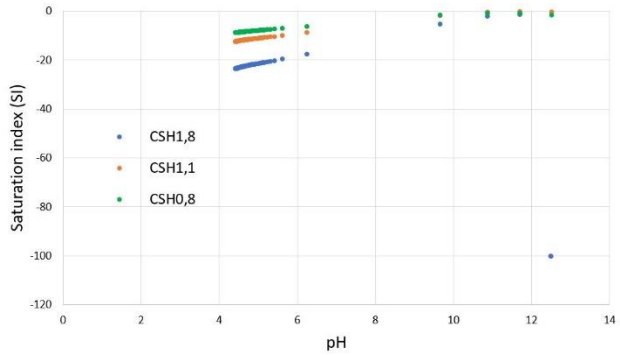

Figure 15. Simulation of the dissolution/precipitation of C-S-H following carbonation

4 CONCLUSIONS

Thermogravimetric analyses (TGA) proved that the matrix became gradually depleted of portlandite during the 28 days of carbonation until exhaustion and enriched in calcium carbonate, thus indicating the total transformation of this hydrate to calcite. The dosage of these minerals by TGA and their identification and semi-quantification by X-ray diffraction analysis (XRD) confirmed these phase changes. TGA also revealed that the production of calcite was supported by C-S-H decalcification after the 14th day of carbonation and after CH degradation.

In conclusion, carbonation induced a decrease in the pH of S/S treated soil causing the total decomposition of portlandite and its conversion into calcium carbonate. Participation of C-S-H in producing this mineral has also been proven. Geochemical modeling of the carbonation of monoliths using PHREEQC showed a decrease in monolith pH, an increase in the calcium, silicon and aluminum concentrations in solution because of the dissolution of the portlandite and the anhydrous tricalcium aluminate and the decalcification of C-S-H. Calcium concentration decreased

with the acidification of the solution because of calcium carbonate precipitation. Silicon concentration has been stabilized in acidic medium because of the formation of silica gel by the C-S-H carbonation. The immobilization of lead by carbonation was also shown.

Acknowledgements

This work was supported by the Natural Sciences and Engineering Research Council of Canada (NSERC). We would like to express our sincere thanks to the following ÉTS and UQAM technicians: S. Menard, M. Dubois, A. Vadeboncoeur and G. Chamoulaud. The help of Mirela Sona and Valeri Mambilo Ondo is gratefully acknowledged.

References

Antemir, A., Hills, C. D., Carey, P. J., Gardner, K. H., Bates, E. R. and A. K. Crumbie. 2010. Long-term performance of aged waste forms treated by stabilization/solidification, *Journal of Hazardous Materials,* 181: 65-73.

Appelo, C. A. J. and D. Postma (2005). *Geochemistry, groundwater and pollution* (2nd edition éd.). Balkema.

ASTM International. *Standard practice for making and curing concrete test specimens in the laboratory.* International standard, ASTM C192-07, West Conshohocken (PA): ASTM, 2007, 8 p.

Bertos, M. F., S. J. R. Simons, C. D. Hills et P. J. Carey. 2004. A review of accelerated carbonation technology in the treatment of cement-based materials and sequestration of CO2. *Journal of Hazardous Materials*, 112: 193-205.

Bonen, D. and S. L. Sarkar. 1995. The superplasticizer adsorption capacity of cement pastes, pore solution composition, and parameters affecting flow loss. *Cement and Concrete Research*, 25: 1423-1434.

Bouzahzah, B., V. Yurchenko, F. Nagajyothi, J. Hulit, M. Sadofsky, V. L. Braunstein, S. Mukherjee, H. Weiss, F. S. Machado, R. G. Pestell, M. P. Lisanti, H. B. Tanowitz and C. Albanese. 2008. Regulation of host cell cyclin D1 by Trypanosoma cruzi in myoblasts. *Cell Cycle,* 7: 500-503.

Bozkurt, S., L. Moreno and I. Neretnieks. 2000. Long-term processes in waste deposits. *Science of the Total Environment,* 250: 101-121.

Cazalet, M. L. 2012. Caractérisation physico-chimique d'un sédiment marin traité aux liants hydrauliques. Évaluation de la mobilité potentielle des polluants inorganiques. *Chimie, Procédés, Environnement de Lyon.*

Chao, S., J. Liqin and Z. Wenjun. 2014. A review on heavy metal contamination in the soil worldwide: Situation, impact and remediation techniques. *Environmental Skeptics and Critics,* 3: 24-38.

Chen, Q., Zhang, L., Ke, Y., Hills, C., Kang and Y. 2009. Influence of carbonation on the acid neutralization capacity of cements and cement-solidified/stabilized electroplating sludge, *Chemosphere,* 74: 758-764.

Conner, J. R., Li. A. Cotton and S. 1990. Stabilization of hazardous waste landfill leachate treatment residue, *Journal of Hazardous Materials,* 24: 111-121.

Dunster, A. M. 1989. An investigation of the carbonation of cement paste using trimethylsilylation. *Advances in Cement Research,* 2: 99-106.

Duprat, F., Tru, V. N. and A. Sellier. 2014. Accelerated carbonation tests for the probabilistic prediction of the durability of concrete structures, *Construction and Building Materials,* 66: 597-605.

El Bedoui, S., F. Duhaime and J. S. Dubé. 2017. Influence of carbonation on the release of arsenic and lead from cementitious matrices. In 70th Annual Canadian Geotechnical Conference = 70ème Conférence Annuelle Canadienne de Géotechnique (Ottawa, Canada, Oct. 01-04, 2017) Canadian Geotechnical Society = Société canadienne de géotechnique.

Groves G. W., D. I. Rodway et I. G. Richardson. 1990. The carbonation of hardened cement pastes. *Advances in Cement research,* 3: 117-125.

Gunning, P. J., C. D. Hills et P. J. Carey. 2010. Accelerated carbonation treatment of industrial wastes. *Waste Management,* 30 :1081-1090.

Lange, L. C., Hills, C. D. and A. B. Poole. 1996. The influence of mix parameters and binder choice on the carbonation of cement solidified wastes, *Waste Management,* 16: 749-756.

Morandeau, A. 2014. « Carbonatation atmosphérique des systèmes cimentaires à faible teneur en portlandite ». Civil Engineering. *Université Paris-Est.*

Peyronnard, O. 2008. « Apports méthodologiques pour la modélisation du comportement à la lixiviation de résidus minéraux. Application aux solidifiats de boues d'hydroxydes métalliques ». *L'Institut National des Sciences Appliquées de Lyon*.

Šavija, B. and M. Lukovic. 2016. Carbonation of cement paste: Understanding, challenges, and opportunities. *Construction and Building Materials,* 117: 285-301.

Scordia, P. Y. 2008. « Caractérisation et valorisation de sédiments fluviaux pollués et traités dans les matériaux routiers ». *École centrale de Lille*.

Song, S. M., Wei, C. X., Liu, Y. 2006. Durability of the reactive powder concrete, *International Symposium on Concrete Technology for Sustainable Development,* 1 and 2: 1139-1145.

Stronach, S. A., N. L. Walker, D. E. Macphee and F. P. Glasser. 1997. Reactions between cement and As(III) oxide: The system CaO-SiO2- As2O3-H2O at 25C. Waste Management, 17: 9-13.

Thiery, M. 2006. *Modélisation de la carbonatation atmosphérique des matériaux cimentaires : prise en compte des effets cinétiques et des modifications microstructurales et hydriques*, PhD Thesis, Laboratoire central des ponts et chaussées, Paris, France.

Wang, P., Q. Xue, J. S. Li and T. T. Zhang. 2016. Effects of pH on leaching behavior of compacted cement solidified/stabilized lead contaminated soil, *Environmental Progress & Sustainable Energy,* 35: 149-155.